



Thermodynamic Simulation of an Efficient Flash Ironmaking Technology for Chadormalu Mining and Industrial Company

F. Firouzi, S. K. Sadrnezhad*

Department of Materials Science and Engineering, Sharif University of Technology, Tehran, Iran

PAPER INFO

Paper history:

Received 21 June 2023

Received in revised form 16 October 2023

Accepted 27 October 2023

Keywords:

Flash Ironmaking

Chadormalu Concentrate

Thermodynamic Simulation

Heat and Material Balances

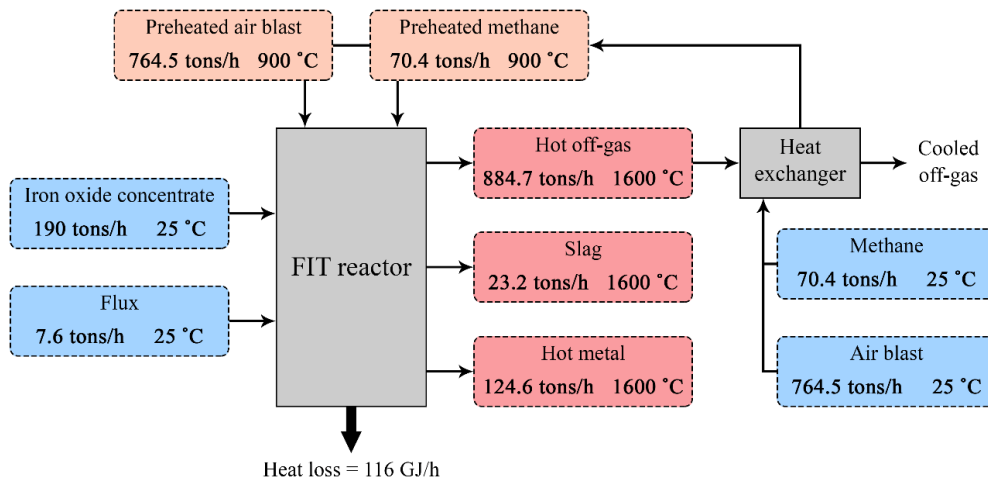
CO₂ Emission

ABSTRACT

The Flash Ironmaking Technology (FIT) utilizing methane (CH₄) and air blast (containing 21% oxygen) has been exclusively simulated and calculated for the Chadormalu Mining and Industrial Company (CMIC). The obtained results based on thermodynamic simulation and heat and material balance calculations of the FIT have revealed that a total rate of 70.405 tons/h preheated CH₄ is required for the annual production of one million tons of hot metal with 95% metallization. 47% of the methane acts as a reducing agent, and the rest burns with 764.489 tons/h preheated air blast (including 20% excess) to provide 1078 GJ/h energy for running the process at 1600 °C (1873 K). Accordingly, 193.134 tons/h carbon dioxide (CO₂) is emitted through the process, equivalent to 1.550 tons for every ton of produced hot metal. It indicates that the simulated FIT is eco-friendlier than the blast furnace and coal-based direct reduction ironmaking processes while eliminating coke-making, pelletization or gas-reforming units.

doi: 10.5829/ije.2024.37.05b.17

Graphical Abstract



1. INTRODUCTION

Crude steel is the most consuming construction material, with a worldwide production of 1885 million tons in 2022 (1). Despite the development of different ironmaking technologies, the blast furnace is still the

most dominant, supplying about 75% of the world's iron (2). The rest includes direct reduction processes, categorized into gas- and coal-based types (3). In 2022, over 127 million tons of direct reduced iron (DRI) were produced all over the world, about 70% of them via gas-based reduction processes, such as MIDREX (57.8%)

*Corresponding Author: sadrnez@sharif.edu (S. K. Sadrnezhad)

and HYL/Energiron (12.1%). Rotary kiln and PERED are coal-based processes that accounted for 27.9% and 2.2% of the total DRI production, respectively (4).

The blast furnace benefits from coke, reducing agents' supplier and fuel for achieving high temperatures. Despite its dominance, ironmaking via the blast furnace method has many drawbacks. The process is strongly dependent on good quality coke, which its short supply has made it expensive all around the world. Establishing a coke oven and pelletization/sintering plants are also required for blast furnace ironmaking (5-8). On the other hand, various technologies developed for DRI production utilize lower-temperature operations (9, 10). These processes, however, suffer from some technical and operational problems. Freshly produced DRI is highly reactive and extremely susceptible to oxidation in the ambient atmosphere. Hence, its handling and storage are always a great concern of direct reduction plants (11, 12). Unintentional sticking and agglomeration of iron ore pellets during reduction, mainly due to building up of low melting eutectic phase and partial sintering, disturbs the continuous operation (13, 14). The employed aluminosilicate refractories are vulnerable to destruction by steam, H₂, and CO attack, and carbon deposition in the liner pores (15). Furthermore, emissions of carbon oxides from all discussed ironmaking processes are significant, which leads to serious environmental problems, primarily global warming (16-19). Considering the technical shortcomings of current methods and global environmental issues, more energy-efficient and eco-friendly ironmaking technologies need to be developed.

A novel flash ironmaking technology (FIT) has recently been developed, similar to the copper flash smelting processes (20). FIT is based on directly reducing iron oxide concentrate by a gaseous reducing agent (such as hydrogen or natural gas) through a gas-solid suspension reaction (21-23). As schematically depicted in Figure 1, fine iron oxide concentrate and flux particles are sprinkled into the flash ironmaking reactor with preheated feed gas and oxygen. A part of the feed gas burns with oxygen to sustain the reactor temperature of 1500-1600 °C (1773-1873 K). The rest reduces input iron oxides in the presence of flux, producing molten iron (hot metal) and fused slag of oxide constituents. They are given enough time to undergo a gravitic separation among the settlement region. Moreover, hot off-gas (containing H₂, H₂O, CO, and CO₂) is directed toward the heat exchanger to preheat the feed gas (24-26).

The novel FIT directly utilizes the fine particles of iron oxide concentrate (<100 μm) without further treatment, resulting in very high reaction rates. Hence, high metallization degrees can be achieved within a few seconds of the residence time (27-29). The process is flexible with a wide variety of gaseous reducing agents, including natural gas (23, 24), hydrogen (H₂) (27-30), carbon monoxide (CO) (31-33), methane (CH₄) (34) or

their mixture. Although pure oxygen or oxygen-enriched air is regularly used for fuel combustion to reduce emissions (24, 34), the process can utilize air blast instead, which is more economical. In addition, highly problematic coke-making, pelletization/sintering, and gas-reforming units would be eliminated (24-26). A typical FIT process is reported to emit less than 0.98 tons of CO₂ and consumes about 8.68 GJ energy for every ton of hot metal produced, which are believed to be, respectively, about 39% and 32% lower than the average amounts corresponding to the conventional blast furnace ironmaking process (24).

This study aims to implement a thermodynamic simulation of the FIT exclusively for iron oxide concentrate produced by the Chadormalu Mining and Industrial Company (CMIC), known as one of the leading suppliers of iron oxide concentrate in Iran and the Middle East (35). First, the process progression is predicted and discussed according to the simulated equilibrium compositions for the increasing input rate of methane as the only reducing agent. The rates of fuel and air blast (containing 21% oxygen, as a new option for fuel combustion in the FIT) are calculated based on the heat and material balances for achieving 95% metallization. Furthermore, the process emissions are calculated and compared with those of the conventional ironmaking processes.

2. METHODOLOGY

The FIT thermodynamic simulation and relevant calculations were performed based on the annual production of one million tons of hot metal. The chemical composition of the Chadormalu iron oxide concentrate and the intended flux are presented in Tables 1 and 2, respectively. The iron content of concentrate, coupled with 320 days of operation, resulted in its input rate of 190 tons/h. Furthermore, the input rate of flux was considered one-twenty-fifth of the concentrate rate (i.e., 7.6 tons/h).

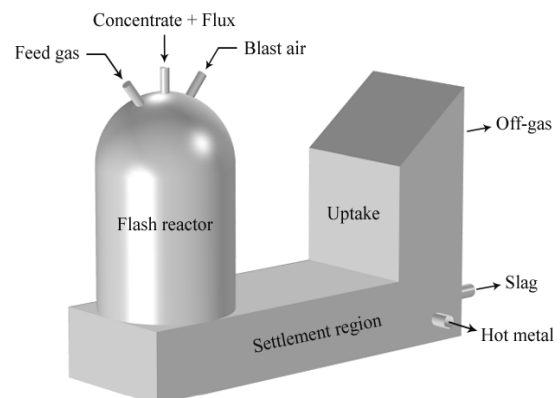


Figure 1. A schematic representation of the flash ironmaking technology (FIT)

TABLE 1. Chemical composition of the Chadormalu iron oxide concentrate (36)

Component	Content (wt.%)
Fe ₃ O ₄	72.1
Fe ₂ O ₃	24.1
SiO ₂	2.60
CaO	0.45
Al ₂ O ₃	0.40
MgO	0.35

TABLE 2. Chemical composition of the flux

Component	Content (wt.%)
MgO	72.1
CaO	24.1
SiO ₂	2.60

This study benefitted the HSC Chemistry 6.0 software for performing all thermodynamic simulations and relevant calculations based on the heat and material balances. The “Equilibrium Compositions” module was utilized to simulate the process by calculating the equilibrium value of compounds at a specific condition. First, the chemical system was defined by introducing the substances and potentially stable phases to be considered in the “Species” sheet calculations. The amounts of raw materials were inserted based on previously mentioned input rates and chemical compositions. Since investigating the role of methane in the FIT was desired, an initial input amount of 1E-16 Mmol (actually zero) and an incremental step of 0.015 Mmol were selected for this compound. At last, the equilibrium temperature of 1600 °C (1873 K), the total pressure of 1 bar (100 kPa), and 250 steps were applied in the “Options” sheet. It is worth mentioning that the temperature of raw materials did not affect the final equilibrium conditions.

In the next step, heat and material balances were performed to calculate the required amount of methane, air blast, and process emissions using the corresponding module. For this purpose, after selecting the intended equilibrium among 250 previously calculated ones, its corresponding initial value of reactants and equilibrium value of products (including unreacted reactants) were transferred to IN1 and OUT1 sheets of the “Heat and Material Balances” module, respectively. All input streams were at room temperature 25 °C (298 K), except the feed gas (methane) and air blast. Similar to previous works, these streams were justifiably set to be preheated to 900 °C (1173 K) by passing through a heat exchanger (21, 24). The temperature of all output streams would be 1600 °C (1873 K), i.e., the process temperature.

Moreover, a heat loss rate of 116 GJ/h was selected, according to the evident data given in the literature (24).

It is noteworthy to mention that previous calculations did not consider the constituents involved in fuel combustion. Thus, the amount of methane required for heat generation in the process and the combustion products were related to the molar value of air blast (containing 21% O₂ and 79% N₂) to satisfy the material balance. Excess air blast was also considered in calculations to ensure complete fuel combustion. The input value of the blast’s oxygen was the independent parameter that the module iterations would finally determine it to achieve the heat balance.

3. RESULTS AND DISCUSSION

3. 1. Process Progression Figure 2 represents different molar equilibrium compositions for the increasing rate of CH₄. Every set of points located on an imaginary vertical line represents an individual equilibrium for a specific input rate of CH₄. Therefore, the reduction progression can be described by putting together all 250 different equilibriums based on an operation time of one hour. Partial reductions start with converting hematite (Fe₂O₃) and magnetite (Fe₃O₄) in the feedstock to their relevant lower oxides. Therefore, the equilibrium value of Fe₂O₃ decreases continuously. However, simultaneous production and reduction of Fe₃O₄ result in a slight increase in its equilibrium value, followed by a descending trend.

Afterward, the equilibrium value of wustite (FeO) rises steeply, reaching a maximum of 2.135 Mmol for 0.390 Mmol of input CH₄. For this input amount of CH₄, metallic iron starts to be produced, and its equilibrium value gradually increases at the expense of FeO

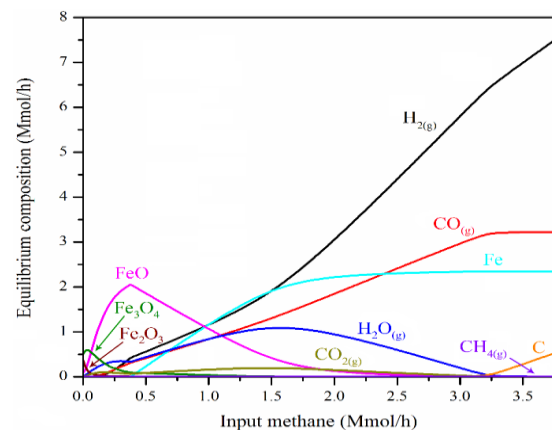
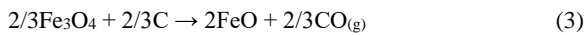
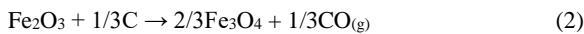


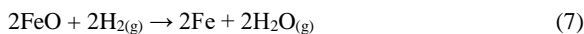
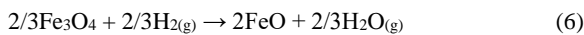
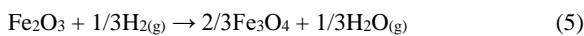
Figure 2. Different equilibrium compositions of the FIT for the increasing rate of methane at 1600 °C (1873 K). Each graph is obtained by putting together the results of 250 different equilibriums.

diminishing. Finally, the equilibrium value of molten iron reaches its maximum amount of 2.348 Mmol by completing FeO reduction (for 3.450 Mmol of input CH₄). Flux or other oxide constituents in concentrate (i.e., CaO, SiO₂, MgO, and Al₂O₃) do not affect the equilibrium processes. They are heated to the operating temperature and form a fused slag. Thus, their different contents in various operating units do not affect the discussed process progression.

It is also worth spending a few sentences on gaseous constituents to cognize the process better. Production of carbon oxides and water vapor through the process can be attributed to the reduction of iron oxides by the carbon and hydrogen contents of methane, respectively. A continuous increase in the equilibrium value of CO indicates that the carbon content of methane is thoroughly involved in all partial reductions, according to Reactions 1 to 4. This proposition is confirmed by considering negligible equilibrium values of CO₂ and stable carbon throughout the process, together with stable carbon (soot) formation for keeping methane feeding after the completion of reductions.



On the other hand, partial reductions by the hydrogen content of methane (produced through Reaction 1) occur according to Reactions 5 to 7. The variation trend of equilibrium H₂O reveals that for an increasing amount of input methane, the contribution of hydrogen in partial reductions increases gradually, reaching its maximum for 1.575 Mmol CH₄. Further increase in the input amount of methane gradually decreases the contribution of hydrogen in the reduction process.



Besides using fine particles of concentrate, the hydrogen contribution in reductions is another reason for high reaction rates in the FIT because it is well-known that iron oxide reduction by hydrogen is more favorable than by CO from thermodynamics and kinetics viewpoints. Unlike CO, hydrogen reduction of iron oxides are more endothermic and thermodynamically proceeds more efficiently at higher temperatures (37). On the other hand, smaller atomic size of hydrogen and higher diffusivity make H₂ a faster reducing agent comparing to CO (38). Hydrogen participation in partial reductions also improves the process eco-friendliness

through decreasing methane consumption, which lowers the subsequent carbon oxide emissions (27-30, 39).

3. 2. Heat and Material Balances The results of heat and material balances of the FIT are utilized for calculating the required feed gas, air blast, and carbon oxides emissions. For this purpose, the equilibrium representing 95% metallization for 2.07 Mmol/h of input CH₄ is selected among the others. As the “Equilibrium Compositions” module calculates the thermodynamic equilibrium condition, the calculated rate of input CH₄ is just the theoretical one needed for achieving the equilibrium. In such a case, the preliminary results (refer to supplementary Table S1) indicate that the lack of 1078 GJ/h energy (8.65 GJ per ton of hot metal) disturbs the heat balance of the process. Therefore, a further CH₄ is also needed as fuel to burn with air blast for heat generation through complete or incomplete combustion (Reactions 8 or 9, respectively). Complete fuel combustion through Reaction 9 can be achieved by introducing excess air blast. The fuel combustion may be considered an individual unit process rather than being coupled with partial reductions to avoid its involved gaseous constituents disrupt the equilibrium conditions of the primary FIT process.

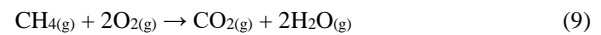


Table 3 represents the final results of heat and material balance calculations (also refer to supplementary Table S2 for complementary information). According to the

TABLE 3. The results of heat and material balances

Stream	T (°C)	Species	Rate ^a (tons/h)	Rate (Mmol/h)	Enthalpy ^b (GJ/h)
Iron oxide concentrate (Input)	25	Fe ₃ O ₄	136.990	0.592	-659.99
		Fe ₂ O ₃	45.790	0.287	-235.99
		SiO ₂	4.940	0.082	-74.89
		CaO	0.855	0.015	-9.68
		Al ₂ O ₃	0.760	0.007	-12.49
		MgO	0.665	0.016	-9.93
Flux (Input)	25	CaO	6.840	0.122	-77.44
		MgO	0.532	0.013	-7.94
		SiO ₂	0.228	0.004	-3.46
Feed gas (Input)	900	CH _{4(g)}	70.405	4.389	-98.68
Air blast (Input)	900	O _{2(g)}	178.063	5.564	160.32
		N _{2(g)}	586.426	20.934	569.48
Hot metal (Output)	1600	Fe	124.629	2.232	168.19

		FeO	8.354	0.116	-17.31
		CaO	7.695	0.137	-76.04
		SiO ₂	5.168	0.086	-68.84
Slag (Output)	1600	MgO	1.197	0.030	-15.51
		Al ₂ O ₃	0.760	0.007	-11.06
		Fe ₃ O ₄	0.037	0.000	-0.11
		Fe ₂ O ₃	0.005	0.000	-0.02
		CO _{2(g)}	107.769	2.449	-758.32
		CO _(g)	54.323	1.939	-113.23
		H ₂ O _(g)	99.938	5.547	-971.92
Off-gas	1600	H _{2(g)}	6.511	3.230	157.06
		O _{2(g)}	29.677	0.927	50.48
		N _{2(g)}	586.426	20.934	1079.94
		CH _{4(g)}	0.000	0.000	0.00
		C (Soot)	0.006	0.001	0.02
Heat loss		-	-	-	116.00

^a This column is used for material balance.

^b This column is used for heat balance. Each given enthalpy contains the heat of formation reaction and the required energy for heating up the compound from 298 K to the specified temperature as well as the values of the latent enthalpies (for possible phase transformations).

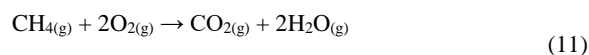
results, running the FIT for the Chadormalu iron oxide concentrate at defined operating conditions consumes 70.405 tons/h CH₄: 47% for iron oxide reductions, and 53% as fuel to provide the mentioned energy required to sustain the system temperature of 1600 °C (1873 K) (refer to electronic supplementary material). Accordingly, 764.489 tons/h air blast including 20% excess (178.063 tons/h O₂ + 586.426 tons/h N₂) is required for complete fuel combustion. Complementary data on different percentages of excess air blast are also presented in supplementary Figure S1.

From the environmental viewpoint, 107.769 tons/h CO₂ and 54.323 tons/h CO are emitted through the simulated FIT. As all CO would eventually be oxidized to CO₂, the process overall emits 193.134 tons/h CO₂. Accordingly, this emission rate accounts for 1.550 tons of CO₂ per ton of hot metal (refer to electronic supplementary material), which implies that the simulated FIT can be categorized among the eco-friendly ironmaking processes. The calculated rate is lower than that of the blast furnace (about 1.700 tons of CO₂ per ton of hot metal) (38) and coal-based direct reduction ironmaking techniques such as rotary kiln (1.391 to 1.880 tons of CO₂ per ton of DRI) and coal gasifier (1.566 to 1.969 tons of CO₂ per ton of DRI) ones (39). This superiority can be generally attributed to the heat generation capacity of carbon (coal or coke) and methane. As Reactions 10 and 11 represent, combustion of each mole of carbon and CH₄ generates 396.2 and 808.9 kJ heat at the operational temperature of 1600 °C (1873 K), respectively. Therefore, elevating the

temperature of constituents consumes less carbon in the form of CH₄, and consequently, less amount of carbon oxide is generated.



$$\Delta H^{\circ}_{1873} = -396.5 \text{ kJ/mol}$$



$$\Delta H^{\circ}_{1873} = -810.1 \text{ kJ/mol}$$

The CO₂ emission of the simulated FIT is only higher than that of the gas-based direct reduction ironmaking techniques emitting 0.815 to 1.160 tons of CO₂ per ton of DRI for the natural gas reformer DRI process (39). However, one should consider the final product of the FIT (molten iron) in return for the solid sponge iron produced by various direct reduction processes which should be further melted by the electric arc furnaces for steelmaking. FIT also eliminates pelletization/sintering and gas-reforming required for DRI production. It is noteworthy that the total CO₂ emission of the intended FIT can be further reduced by substituting the air blast (containing 21% oxygen) with oxygen-enriched air. The more the oxygen content of the air blast is, the eco-friendlier the process would be. Accordingly, the CO₂ emission is reduced to 1.286 tons per ton of hot metal for using pure oxygen in the process (refer to supplementary Table S3). Energy saving strategies such as waste heat recovery and export gases for power generation can further improve the pollution index of the process.

4. CONCLUSIONS

The FIT has been simulated for iron production from the Chadormalu iron oxide concentrate by methane and air blast (containing 21% oxygen). The process eliminates coke-making, pelletization, and gas-reforming units. Based on heat and material balance calculations, 70.405 tons/h CH₄ and 764.489 tons/h air blast (including 20% excess) are required for the annual production of one million tons of hot metal with 95% metallization. Accordingly, methane plays a dual role: 47% as a reducing agent and 53% as fuel to sustain the reactor temperature of 1600 °C (1873 K). Furthermore, 193.134 tons/h CO₂ is emitted, and 1078 GJ/h energy is supplied. The values are equivalent to 1.550 tons of CO₂ and 8.65 GJ energy per ton of hot metal, respectively. Utilizing pure oxygen or oxygen-enriched air blast further improves the pollution index of the simulated FIT and puts it among eco-friendly ironmaking processes.

5. REFERENCES

1. Yearbook SS. World Steel Association: Brussels, Belgium; 2014.
2. Association WS. Fact sheet: energy use in the steel industry. Worldsteel Committee on Economic Studies Brussels, Brussels.

2016. <https://worldsteel.org/wp-content/uploads/Fact-sheet-Energy-use-in-the-steel-industry.pdf>
3. Anameric B, Kawatra SK. Properties and features of direct reduced iron. *Mineral processing and extractive metallurgy review*. 2007;28(1):59-116. <https://doi.org/10.1080/08827500600835576>
 4. World direct reduction statistics. 2023, Midrex Technologies Incorporation: New Jersey, USA. <https://www.midrex.com/wp-content/uploads/MidrexSTATSBook2022.pdf>
 5. Chen Y, Zuo H. Review of hydrogen-rich ironmaking technology in blast furnace. *Ironmaking & Steelmaking*. 2021;48(6):749-68. <https://doi.org/10.1080/03019233.2021.1909992>
 6. Wu X, Wang S, Fang H, Xu Z, Che P, Acquah AK. Study on semi-coke as an alternative fuel for blast furnace injection coal. *Energy Sources, Part A: Recovery, Utilization, and Environmental Effects*. 2022;44(2):5562-73. <https://doi.org/10.1080/15567036.2022.2027577>
 7. Xing X. Effects of coal interactions during cokemaking on coke properties under simulated blast furnace conditions. *Fuel Processing Technology*. 2020;199:106274. <https://doi.org/10.1016/j.fuproc.2019.106274>
 8. Helle H, Helle M, Saxen H. Nonlinear optimization of steel production using traditional and novel blast furnace operation strategies. *Chemical Engineering Science*. 2011;66(24):6470-81. <https://doi.org/10.1016/j.ces.2011.09.006>
 9. Sadrnezhad S. Direct Reduced Iron an Advantageous Charge Material for Induction Furnaces. *International Journal of Engineering*. 1990;3(1):37-48. https://www.ije.ir/article_71018.html
 10. Zare Ghadi A, Valipour M, Biglari M. Transient entropy generation analysis during wustite pellet reduction to sponge iron. *International Journal of Engineering, Transactions B: Applications*. 2018;31(8):1274-82. <https://doi.org/10.5829/ije.2018.31.08b.16>
 11. Paswan MK, Mukherjee C. Economic analysis of transportation directly reduced iron (dri) through ship. *International Journal of Services Technology and Management*. 2012;17(2-4):251-66. <https://doi.org/10.1504/IJSTM.2012.048540>
 12. Towhidi N. Reoxidation rate of sponge iron pellets, briquettes and iron powder compressed to various compressions in air. *International Journal of Engineering*. 1988;1(2):111-6. https://www.ije.ir/article_70983.html
 13. Komatina M, GUDENAU HW. The sticking problem during direct reduction of fine iron ore in the fluidized bed. *Metallurgical and Materials Engineering*. 2018. <https://doi.org/10.30544/378>
 14. Yi L, Huang Z, Jiang T. Sticking of iron ore pellets during reduction with hydrogen and carbon monoxide mixtures: behavior and mechanism. *Powder Technology*. 2013;235:1001-7. <https://doi.org/10.1016/j.powtec.2012.11.043>
 15. Chakraborty I, Sinha S. Refractories for Direct Iron Reduction Processes. https://www.researchgate.net/profile/Indra-Chakraborty-3/publication/344770108_OPTIMISATION_OF_BLAST_FURNACE_TROUGH_LINING_REFRACTORY_PERFORMANCE/links/614c1ee0519a1a381f796959/OPTIMISATION-OF-BLAST-FURNACE-TROUGH-LINING-REFRACTORY-PERFORMANCE.pdf
 16. Gielen D, Moriguchi Y. CO₂ in the iron and steel industry: an analysis of Japanese emission reduction potentials. *Energy policy*. 2002;30(10):849-63. [https://doi.org/10.1016/S0301-4215\(01\)00143-4](https://doi.org/10.1016/S0301-4215(01)00143-4)
 17. Li X, Sun W, Zhao L, Cai J. Material metabolism and environmental emissions of BF-BOF and EAF steel production routes. *Mineral Processing and Extractive Metallurgy Review*. 2018;39(1):50-8. <https://doi.org/10.1080/08827508.2017.1324440>
 18. Dahui XX, Wang. Reducing greenhouse gas emissions from energy consumption activities by the iron and steel industry in East China. *Energy sources*. 1999;21(6):541-6. <https://doi.org/10.1080/00908319950014669>
 19. Zhang X, Jiao K, Zhang J, Guo Z. A review on low carbon emissions projects of steel industry in the World. *Journal of cleaner production*. 2021;306:127259. <https://doi.org/10.1016/j.jclepro.2021.127259>
 20. Kemori N, Denholm W, Kurokawa H. Reaction mechanism in a copper flash smelting furnace. *Metallurgical and Materials Transactions B*. 1989;20:327-36. <https://doi.org/10.1007/BF02696985>
 21. Sohn HY, Mohassab Y. Development of a novel flash ironmaking technology with greatly reduced energy consumption and CO₂ emissions. *Journal of Sustainable Metallurgy*. 2016;2:216-27. <https://doi.org/10.1007/s40831-016-0054-8>
 22. Sohn HY, Fan D-Q, Abdelghany A. Design of novel flash ironmaking reactors for greatly reduced energy consumption and CO₂ emissions. *Metals*. 2021;11(2):332. <https://doi.org/10.3390/met11020332>
 23. Abdelghany A, Fan D-Q, Sohn H. Novel flash ironmaking technology based on iron ore concentrate and partial combustion of natural gas: a CFD study. *Metallurgical and Materials Transactions B*. 2020;51:2046-56. <https://doi.org/10.1007/s11663-020-01909-6>
 24. Pinegar H, Moats MS, Sohn H. Flowsheet development, process simulation and economic feasibility analysis for novel suspension ironmaking technology based on natural gas: Part 1—Flowsheet and simulation for ironmaking with reformerless natural gas. *Ironmaking & Steelmaking*. 2012;39(6):398-408. <https://doi.org/10.1179/1743281211Y.0000000053>
 25. Wang R-r, Zhang J-l, Liu Y-r, Zheng A-y, Liu Z-j, Liu X-l, et al. Thermal performance and reduction kinetic analysis of cold-bonded pellets with CO and H₂ mixtures. *International Journal of Minerals, Metallurgy, and Materials*. 2018;25:752-61. <https://doi.org/10.1007/s12613-018-1623-6>
 26. Yang Y, Bao Q, Guo L, Wang Z, Guo Z. Numerical simulation of flash reduction in a drop tube reactor with variable temperatures. *International Journal of Minerals, Metallurgy and Materials*. 2022;29(2):228-38. <https://doi.org/10.1007/s12613-020-2210-1>
 27. Chen F, Mohassab Y, Jiang T, Sohn HY. Hydrogen reduction kinetics of hematite concentrate particles relevant to a novel flash ironmaking process. *Metallurgical and Materials Transactions B*. 2015;46:1133-45. <https://doi.org/10.1007/s11663-015-0332-z>
 28. Elzohiery M, Fan D, Mohassab Y, Sohn H. Kinetics of hydrogen reduction of magnetite concentrate particles at 1623–1873 K relevant to flash ironmaking. *Ironmaking & Steelmaking*. 2021;48(5):485-92. <https://doi.org/10.1080/03019233.2020.1819942>
 29. Wang H, Sohn H. Hydrogen reduction kinetics of magnetite concentrate particles relevant to a novel flash ironmaking process. *Metallurgical and Materials Transactions B*. 2013;44:133-45. <https://doi.org/10.1007/s11663-012-9754-z>
 30. Qu Y, Xing L, Wang C, Shao L, Zou Z. Kinetic characterization of flash reduction process of hematite ore fines under hydrogen atmosphere. *International Journal of Hydrogen Energy*. 2020;45(56):31481-93. <https://doi.org/10.1016/j.ijhydene.2020.08.196>
 31. Fan D-Q, Elzohiery M, Mohassab Y, Sohn H. The kinetics of carbon monoxide reduction of magnetite concentrate particles through CFD modelling. *Ironmaking & Steelmaking*. 2021;48(7):769-78. <https://doi.org/10.1080/03019233.2020.1861857>
 32. Fan D, Elzohiery M, Mohassab Y, Sohn H. Rate-enhancement effect of CO in magnetite concentrate particle reduction by H₂+

- CO mixtures. *Ironmaking & Steelmaking*. 2021;48(9):1064-75. <https://doi.org/10.1080/03019233.2021.1915645>
33. Chen F, Mohassab Y, Zhang S, Sohn HY. Kinetics of the reduction of hematite concentrate particles by carbon monoxide relevant to a novel flash ironmaking process. *Metallurgical and Materials Transactions B*. 2015;46:1716-28. <https://doi.org/10.1007/s11663-015-0345-7>
 34. Elzohiery M, Fan D, Mohassab Y, Sohn H. Experimental investigation and computational fluid dynamics simulation of the magnetite concentrate reduction using methane-oxygen flame in a laboratory flash reactor. *Metallurgical and Materials Transactions B*. 2020;51(3):1003-15. <https://doi.org/10.1007/s11663-020-01809-9>
 35. (CMIC), C.M.a.I.C. Products of chadormalu mining and industrial co. 2020 <http://chadormalu.com/en-us/Products>
 36. Tahari MNA, Salleh F, Saharuddin TST, Samsuri A, Samidin S, Yarmo MA. Influence of hydrogen and carbon monoxide on reduction behavior of iron oxide at high temperature: Effect on reduction gas concentrations. *International Journal of Hydrogen Energy*. 2021;46(48):24791-805. <https://doi.org/10.1016/j.ijhydene.2020.06.250>
 37. Heidari A, Niknahad N, Iljana M, Fabritius T. A review on the kinetics of iron ore reduction by hydrogen. *Materials*. 2021;14(24):7540. <https://doi.org/10.3390/ma14247540>
 38. Changqing H, Xiaowei H, Zhihong L, Zhang C. Comparison of CO₂ emission between COREX and blast furnace iron-making system. *Journal of environmental sciences*. 2009;21:S116-S20. [https://doi.org/10.1016/S1001-0742\(09\)60052-8](https://doi.org/10.1016/S1001-0742(09)60052-8)
 39. Nduagu EI, Yadav D, Bhardwaj N, Elango S, Biswas T, Banerjee R, et al. Comparative life cycle assessment of natural gas and coal-based directly reduced iron (DRI) production: A case study for India. *Journal of Cleaner Production*. 2022;347:131196. <https://doi.org/10.1016/j.jclepro.2022.131196>

COPYRIGHTS

©2024 The author(s). This is an open access article distributed under the terms of the Creative Commons Attribution (CC BY 4.0), which permits unrestricted use, distribution, and reproduction in any medium, as long as the original authors and source are cited. No permission is required from the authors or the publishers.



Persian Abstract

چکیده

فرآیند تولید آهن به روش فن آوری فلش با استفاده از گاز متان و هوا (حاوی ۲۱٪ اکسیژن) به طور اختصاصی برای شرکت معدنی و صنعتی چادرملو شبیه سازی و محاسبه شده است. نتایج حاصل بر اساس شبیه سازی ترمودینامیکی و محاسبات مربوط به موازنه جرم و انرژی فرآیند فلش نشان می دهد که در مجموع ۷۰/۴۰۵ tons/h متان پیش گرم برای تولید سالانه یک میلیون تن آهن خام با ۹۵٪ احیاء مورد نیاز است. ۴۷٪ از این مقدار متان به عنوان عامل احیاء اکسیدهای آهن عمل کرده و مابقی با ۷۶۴/۴۸۹ tons/h هوای پیش گرم (با احتساب ۲۰٪ مقدار اضافی) می سوزد تا ۱۰۷۸ GJ/h انرژی مورد نیاز برای اجرای عملیات در دمای ۱۶۰۰ °C را تأمین کند. در همین راستا، ۱۹۳/۱۳۴ tons/h دی اکسید کربن طی فرآیند انتشار می یابد که معادل ۱/۵۵۰ تن به ازای تولید هر تن آهن خام است. این امر نشان می دهد که فرآیند فلش شبیه سازی شده، از لحاظ آلایندگی زیست محیطی، پاکیزه تر از روش های کوره بلند و احیاء مستقیم بر پایه زغال برای تولید آهن است که در عین حال، نیاز به استفاده از واحدهای کک سازی، گندله سازی یا ریفرمیگ گاز را برطرف می نماید.

Supplementary Material

NOTE: Original data files of mechanistic study and heat and material balances (MECHANISM.IGI and H&M.BAL) are also included in the ZIP Electronic Supplementary Materials. Use HSC CHEMISTRY version 6.0 or later for using them.

TABLE S1. The results of heat and material balances by ignoring the fuel combustion process

Type	Stream	Temperature (°C)	Species	Rate (tons/h)	Rate (Mmol/h)	Enthalpy* (GJ/h)
Input	Iron oxide concentrate	25	Fe ₃ O ₄	136.990	0.592	-659.99
			Fe ₂ O ₃	45.790	0.287	-235.99
			SiO ₂	4.940	0.082	-74.89
			CaO	0.855	0.015	-9.68
			Al ₂ O ₃	0.760	0.007	-12.49
			MgO	0.665	0.016	-9.93
	Flux	25	CaO	6.840	0.122	-77.44
			MgO	0.532	0.013	-7.94
	Feed gas	900	SiO ₂	0.228	0.004	-3.46
			CH ₄ (g)	33.208	2.070	-46.54
Total				230.808	3.208	-1138.35
Output	Hot metal	1600	Fe	124.629	2.232	168.19
			FeO	8.354	0.116	-17.31
			CaO	7.695	0.137	-76.04
	Slag	1600	SiO ₂	5.168	0.086	-68.84
			MgO	1.197	0.030	-15.51
			Al ₂ O ₃	0.760	0.007	-11.06
			Fe ₃ O ₄	0.037	0.000	-0.11
			Fe ₂ O ₃	0.005	0.000	-0.02
	Off-gas	1600	CO ₂ (g)	5.727	0.130	-40.30
			CO(g)	54.323	1.939	-113.23
			H ₂ O(g)	16.397	0.910	-159.47
			H ₂ (g)	6.511	3.230	157.06
			CH ₄ (g)	0.000	0.000	0.00
C (Soot)			0.006	0.001	0.02	
<i>Heat loss</i>						116.00
Total				230.808	8.818	-60.62
Balance = Total_{Output} – Total_{Input}				0.000	5.610	1077.73

TABLE S2. Complementary results of heat and material balances

Type	Stream	Temperature (°C)	Rate (tons/h)	Enthalpy* (GJ/h)
Input	Concentrate	25	190.000	-1002.96
	Flux	25	7.600	-88.84
	Feed gas	900	70.405	-98.68
	Air blast	900	764.490	729.79
Total			1032.495	-460.67

	Hot metal	1600	124.629	168.19
	Slag	1600	23.216	-188.88
Output	Off-gas	1600	884.650	-555.98
			<i>Heat loss</i>	116.00
	Total		1032.495	-460.67
Balance = Total_{Output} - Total_{Input}			0.000	0.00

TABLE S3. The results of heat and material balances for using pure oxygen

Type	Stream	Temperature (°C)	Species	Rate (tons/h)	Rate (Mmol/h)	Enthalpy* (GJ/h)
Input	Iron oxide concentrate	25	Fe ₃ O ₄	136.990	0.592	-659.99
			Fe ₂ O ₃	45.790	0.287	-235.99
			SiO ₂	4.940	0.082	-74.89
			CaO	0.855	0.015	-9.68
			Al ₂ O ₃	0.760	0.007	-12.49
			MgO	0.665	0.016	-9.93
	Flux	25	CaO	6.840	0.122	-77.44
			MgO	0.532	0.013	-7.94
	Feed gas	900	SiO ₂	0.228	0.004	-3.46
			CH ₄ (g)	58.449	3.643	-81.92
Pure oxygen	900	O ₂ (g)	120.832	3.776	108.79	
	Total		376.881	8.557	-1064.94	
Output	Hot metal	1600	Fe	124.629	2.232	168.19
			FeO	8.354	0.116	-17.31
			CaO	7.695	0.137	-76.04
	Slag	1600	SiO ₂	5.168	0.086	-68.84
			MgO	1.197	0.030	-15.51
			Al ₂ O ₃	0.760	0.007	-11.06
			Fe ₃ O ₄	0.037	0.000	-0.11
			Fe ₂ O ₃	0.005	0.000	-0.02
			CO ₂ (g)	74.971	1.704	-527.54
	Off-gas	1600	CO(g)	54.323	1.939	-113.23
			H ₂ O(g)	73.087	4.057	-710.79
			H ₂ (g)	6.511	3.230	157.06
			O ₂ (g)	20.138	0.629	34.24
			CH ₄ (g)	0.000	0.000	0.00
			C (Soot)	0.006	0.001	0.02
			<i>Heat loss</i>		116.00	
	Total		376.881	14.168	-1064.94	
Balance = Total_{Output} - Total_{Input}			0.000	5.611	0.00	

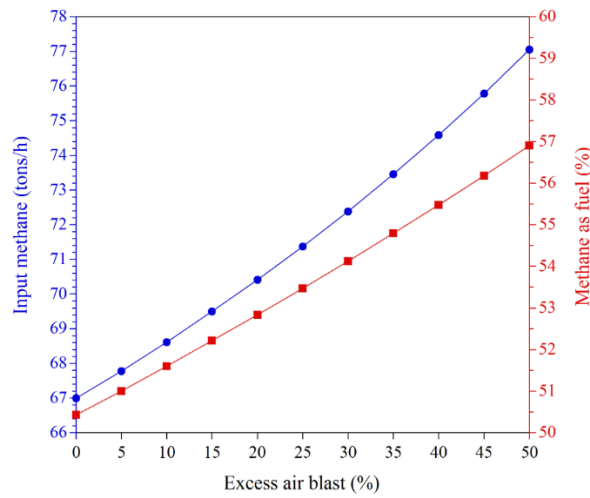


Figure S1. Effect of excess air blast on total input rate of methane (squares) and contribution of methane as fuel (circles)

Clarification of calculations (based on final heat and material balances):

- The degree of metallization $= \frac{n_{\text{Fe (produced)}}}{n_{\text{Fe (max)}}} = \frac{2.232}{2.348} \times 100 = 95\%$
- The methane's contribution as reducing agent $= \frac{n_{\text{CH}_4 \text{ (reducing agent)}}}{n_{\text{CH}_4 \text{ (total)}}} = \frac{2.07}{4.389} \times 100 = 47\%$
- The methane's contribution as fuel $= \frac{n_{\text{CH}_4 \text{ (fuel)}}}{n_{\text{CH}_4 \text{ (total)}}} = \frac{4.389 - 2.07}{4.389} \times 100 = 53\%$
- Energy for every ton of hot metal $= \frac{\text{total energy}}{m_{\text{Fe}}} = \frac{1078}{124.629} = 8.65 \text{ GJ / ton hot metal}$
- CO₂ emission for every ton of hot metal $= \frac{m_{\text{CO}_2} + \left(\frac{M_{\text{CO}_2}}{M_{\text{CO}}}\right)m_{\text{CO}}}{m_{\text{Fe}}} = \frac{107.769 + \left(\frac{44}{28}\right)54.323}{124.629} = 1.550 \text{ tons CO}_2 / \text{ton hot metal}$